

Millimeter Wave Switched Beam Rectangular Loop Dipole Antenna Array Using a 4×4 Butler Matrix

Kunooru Bharath^{1, *}, Srujana Vahini N¹, Rama K. Dasari¹,
Mahesh P. Abegaonkar², and Vijay M. Pandharipande¹

Abstract—A four-stage switched beam antenna array at millimeter-wave (mm-wave) frequencies is designed, fabricated, and experimental results are demonstrated. A novel rectangular loop dipole antenna (RLDA) applying the quasi Yagi-Uda concept is designed to achieve high gain and wide bandwidth with end-fire radiation. This RLDA with director has a return loss better than 10 dB over a frequency range of 32 GHz to 37 GHz and a peak gain of 8.5 dB. The proposed high gain end-fire RLDA antenna in combination with a 4×4 Butler Matrix (BM) creates the switched beam configuration and generates four beams in the directions of $15^\circ \pm 2^\circ$, $-45^\circ \pm 4^\circ$, $38^\circ \pm 2^\circ$, and $-15^\circ \pm 1^\circ$ at 33.5 GHz, 34.5 GHz, and 35.5 GHz with successive input port excitation. The switched beam configuration has overall dimensions at 34.5 GHz is $26 \text{ mm} \times 25.8 \text{ mm}$ ($3.03\lambda \times 3.0\lambda$).

1. INTRODUCTION

High gain antennas with beam tilting capability in the millimetre wave frequency are required to meet the requirements of future wireless communication. These antennas will compensate the losses at high frequencies as well as increase capacity by decreasing co-channel interference [1]. Beam titling can be performed mechanically or electrically. Electronic beam tilting technique uses RF MEMS, varactor diodes, and pin-diodes, which necessitate an additional biasing circuit, resulting in a complex feed system [2]. The mechanical beam tilting technique, on the other hand, involves a sophisticated mechanical framework, which increases the system's size and weight. Furthermore, the aforementioned techniques are too expensive. Researchers have proposed several beam tilting techniques using high refractive index metamaterial (HRIM) [3], frequency selective surface [4], and Asymmetric half bow-tie antenna with V-shape ground [5]. However, in these techniques the physical structure of the antenna should be changed to get the main beam scanned.

Other well-known beamforming methods of switched-beam antenna systems are Blass [6], Nolen matrix [7], Rotman lenses [8], reflector lens [9], and Butler matrices [10]. In beamforming network design, the coherently radiating periodic structures (CORPS) concept [11–13] and the cophasal subarrays concept for concentric ring arrays [14] are used in feed arrangement. These beamforming networks employ time delays caused by varying channel lengths and circuit components to guide beams in predefined directions. The BM is the most often used because of its wideband characteristics and simple form. The switched beam antenna arrangement can provide a discontinuous directional beam tilting capability while requiring low hardware complexity and ease of manufacture.

In switched beam antenna systems (SBAS), radiating element performance plays a vital role in the design of an efficient system at mm-wave frequencies. In the literature, various types of switched beam antenna configurations have been presented using various radiating elements at mm-wave frequencies.

Received 30 October 2021, Accepted 6 January 2022, Scheduled 7 January 2022

* Corresponding author: Kunooru Bharath (bharath.goud3535@gmail.com).

¹ Centre for Excellence in Microwave Engineering, Osmania University, Hyderabad, India. ² Centre for Applied Research in Electronics, IIT Delhi, New Delhi, India.

An inset fed patch antenna array was utilized as a radiating structure to construct a switched-beam antenna system operating at 60 GHz [15], but it has low gain and narrow bandwidth. A highly complex mushroom structure and square ring radiating structure at 35 GHz SBAS is proposed with 7.5 dB gain [16]. A double ridge gap horn array is used as a radiating structure to achieve multibeam capability at 30 GHz [17], and it consumes more space. A seven-element microstrip comb-line array antenna is used as a radiating structure, and it is cascaded with the modified BM to obtain multibeam capability at 28 GHz [18]; however, it consumes more space and covers less band. A 1×8 slot array is used as a radiating structure in a SIW technology based complex dual layer multibeam system at 28 GHz [19]. A 8×10 slot-coupled patch array is used as a radiating structure in a complex three layer multibeam system at 38 GHz, and it has less beam steering [20].

While incorporating switched beam mechanism to the antenna, the overall size of the structure is increased in terms of area and number of layers utilized. In this work, we focus on these limitations including the narrow-band performance. To improve overall performance of the switched beam system, we design a novel wideband high gain end-fire rectangular loop dipole antenna (RLDA) with the quasi Yagi-Uda concept used as a radiating structure, which is cascaded with a 4×4 Butler matrix to form a switched beam antenna system at mm-wave frequencies. To ensure the validity of the results, switched beam antenna is fabricated, and measured results are presented with simulation data.

2. RECTANGULAR LOOP DIPOLE ANTENNA (RLDA) WITH DIRECTORS

The printed rectangular loop dipole antenna (RLDA) is depicted in Fig. 1(a). Each arm is $\lambda/(4\sqrt{\epsilon_r})$ in length and comprises two rectangular loops (RL1 & RL2) of dissimilar dimensions that are put on the top and bottom faces of a 10 mil thick RT-5880 dielectric substrate. The antenna is matched with the feed line by using an impedance matching transformer. The antenna's rectangular loops (RL1 & RL2)

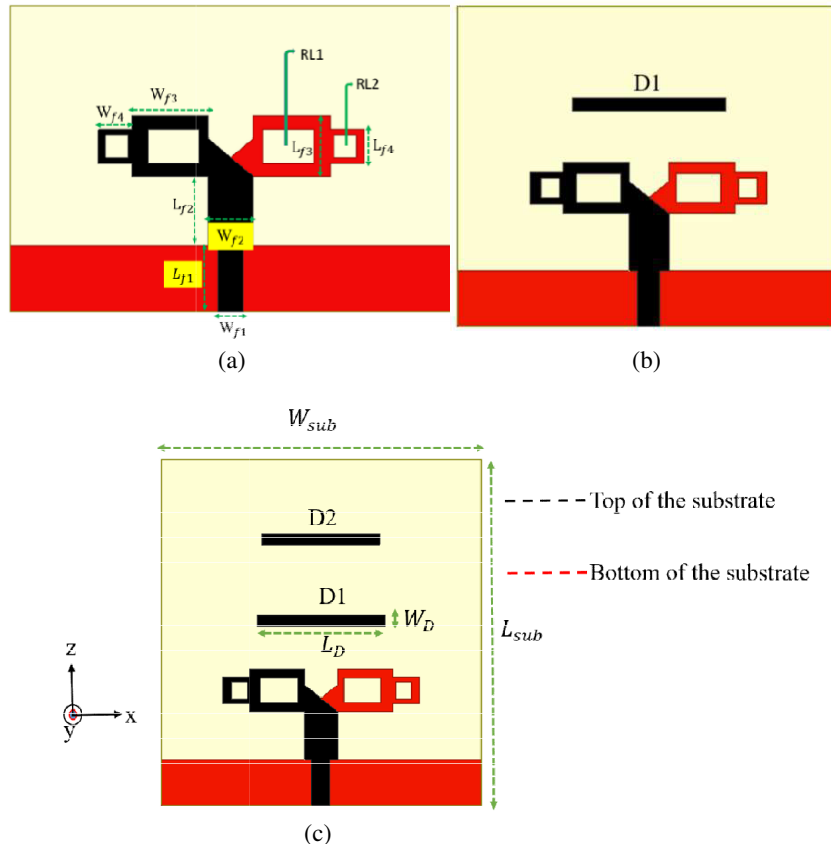


Figure 1. (a) RLDA. (b) RLDA with one director. (c) RLDA with two directors.

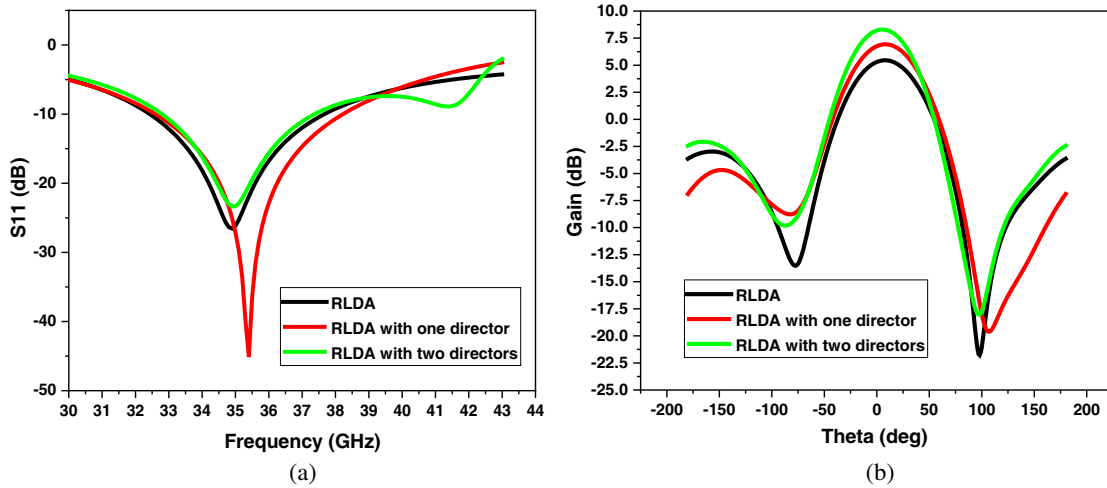


Figure 2. (a) Return loss. (b) Gain pattern in the E -plane.

are utilized to increase the length of current path. In order to improve the gain of the RLDA, directors (D1 & D2) are placed along the radiation direction as seen in Figs. 1(b) & 1(c). The dimensions of the structure are $L_{f1} = 0.61$ mm, $L_{f2} = 0.9$ mm, $L_{f3} = 0.8$ mm, $L_{f4} = 0.5$ mm, $L_{sub} = 6.5$ mm, $W_D = 0.2$ mm, $W_{f1} = 0.35$ mm, $W_{f2} = 0.62$ mm, $W_{f3} = 1.04$ mm, $W_{f4} = 0.5$ mm, $W_{sub} = 6$ mm, and $L_D = 2.3$ mm. The simulated return loss for RLDA and RLDA with directors is below 10 dB over the frequency band of 32–37 GHz as seen from Fig. 2(a). The gain in the E -plane at 34.5 GHz is as seen from Fig. 2(b). For antenna design and optimization, Ansys HFSS is utilized.

3. BUTLER MATRIX (BM) DESIGN

As shown in Fig. 3(a), the block schematic consists of two 45° phase shifters, four 90° couplers, and two crossovers that form a 4×4 BM. Port1–Port4 are the input ports, while Port5–Port8 are the output ports that are connected to the array antenna. By stimulating one of the input ports, progressive phases of $\pm 45^\circ$ and $\pm 135^\circ$ can be achieved at the output ports in this arrangement. The simulated S -parameters of the 4×4 Butler matrix when input ports are excited simultaneously are shown in Fig. 4. When Port1 is stimulated, the isolation and return loss values are better than 22 dB throughout

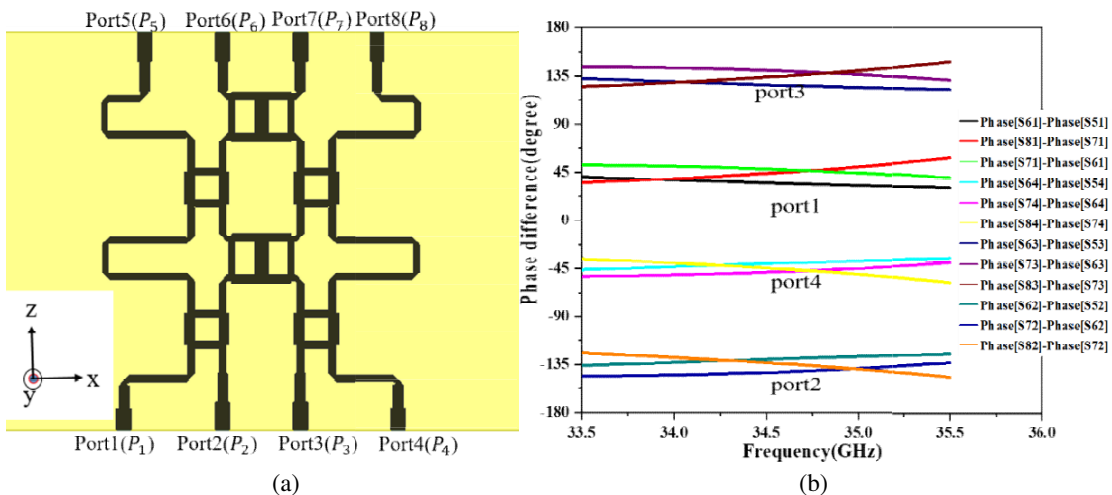


Figure 3. (a) Butler matrix. (b) Phase differences when different ports excited.

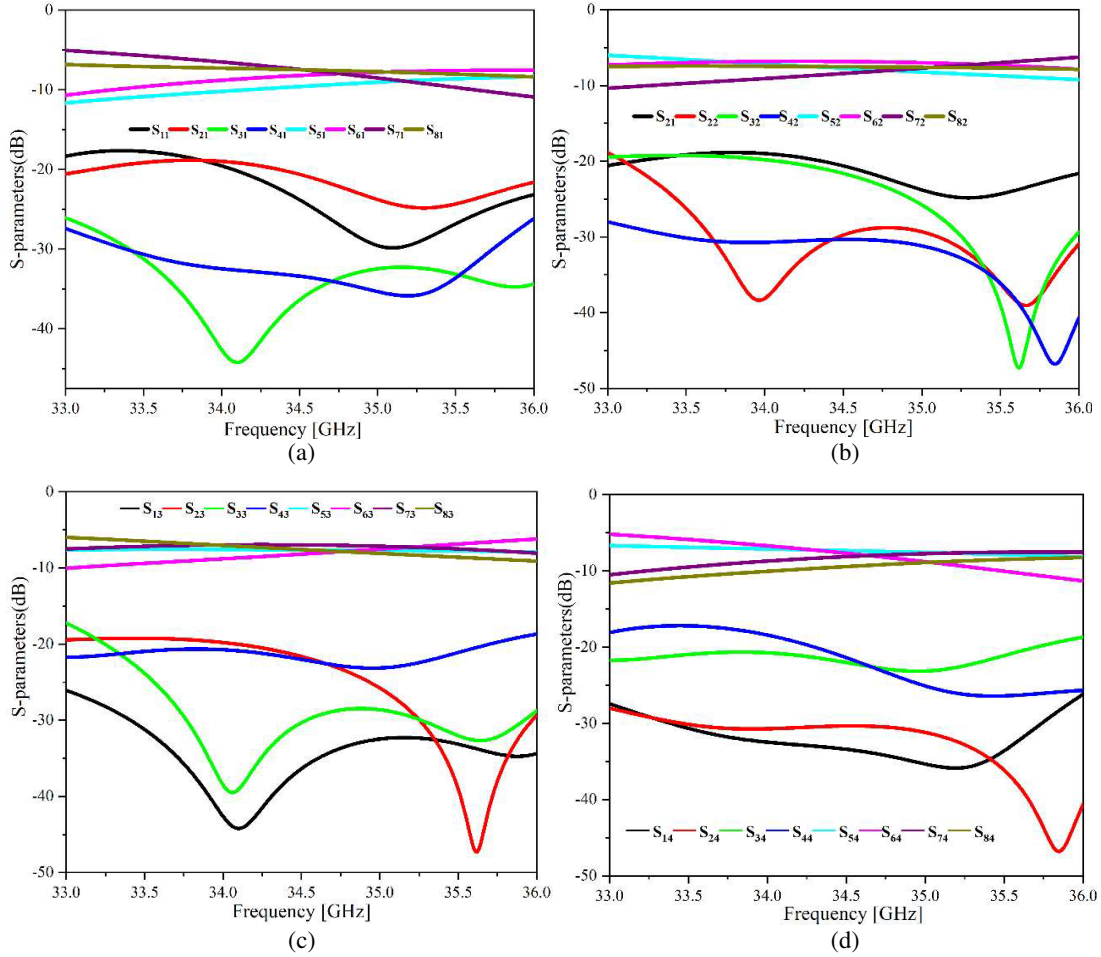


Figure 4. S -parameters with respective input port excitation. (a) P_1 . (b) P_2 . (c) P_3 . (d) P_4 .

the 33.5–35.5 GHz frequency band. The calculated transmission coefficients from Port1 to output ports Port5–Port8 at 35 GHz are -8.12 , -6.52 , -6.81 , and -8.38 dB, respectively. Similarly, when Port2 is stimulated, the reflection and isolation values are better than 21 dB throughout the 33.5–35.5 GHz frequency band. The calculated transmission coefficients from Port1 to output ports Port5–Port8 at 35 GHz are -7.53 , -6.93 , -6.854 , and -7.45 dB, respectively. Similarly, when Port3 is stimulated, the isolation and reflection values are better than 20.4 dB throughout the 33.5–35.5 GHz frequency band. The calculated transmission coefficients from Port1 to output ports Port5–Port8 at 35 GHz are -7.33 , -7.15 , -7.72 , and -8.05 dB respectively. Similarly, when Port4 is stimulated, the isolation and reflection values are better than 22 dB throughout the 33.5–35.5 GHz frequency band. The calculated transmission coefficients from Port1 to output ports Port5–Port8 at 35 GHz are -6.82 , -7.37 , -7.53 , and -7.85 dB, respectively. Fig. 3(b) depicts the simulated phase differences between two neighbouring output ports, namely Phase(S6P)-Phase(S5P), Phase(S7P)-Phase(S6P), and Phase(S8P)-Phase(S7P). For Port1–Port4 excitation, the relative phase development between two adjacent output ports is $+45^\circ$, -135° , $+135^\circ$, and -45° , respectively. When Port1 to Port4 are stimulated, a maximum simulated phase error of about 10° is detected as compared to the theoretical phase shift over the frequency range of 33.5–35.5 GHz.

4. RESULTS AND DISCUSSION

Figure 5 shows the theoretical phase difference between adjacent output ports of BM when P_1 to P_4 are excited respectively. The phase differences are applied to the antenna elements to produce beam

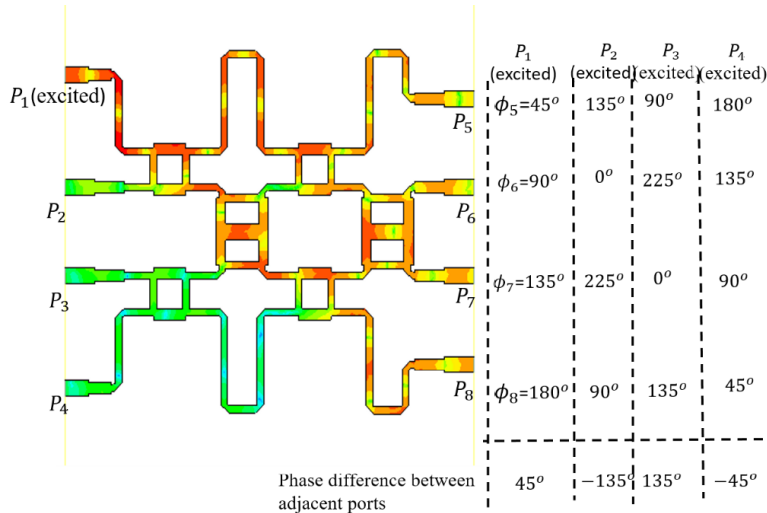


Figure 5. Field distribution of Butler matrix when Port1 excited.

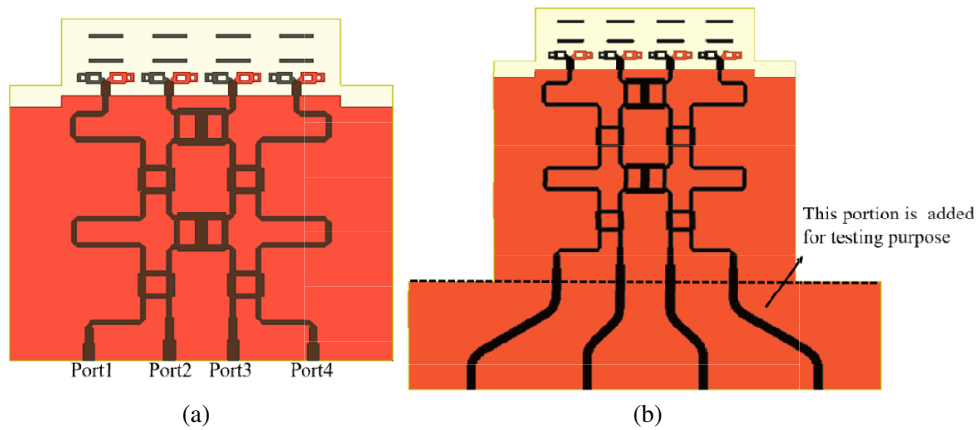


Figure 6. (a) Simulated structure of RLDA array with Bulter matrix. (b) Extra portion added for testing purpose.

Table 1. Beam tilt calculations.

Excited Port	Phase shift between antenna elements (γ)	Main Beam Direction (Scan Angle) $\theta = \text{arc Sin}(\gamma\lambda/2\pi d)$
P_1	45°	15°
P_2	-135°	-45°
P_3	135°	45°
P_4	-45°	-15°

tilt. The beam directions are determined according to the formulas in Table 1. The simulated structure of switched beam configuration is shown in Fig. 6, Port1 to Port4 are input ports, while Port5 to Port8 are output ports of the BM that connect to the rectangular loop dipole antenna (RLDA) array. A phase difference of $+45^\circ$ and -45° exists between neighbouring antenna elements when Port1 and Port4 are excited, resulting in the tilt of the main beam of the antenna to $+15^\circ$ and -15° in the E -plane with respect to end-fire direction. Similarly, a phase difference of -135° and $+135^\circ$ exists between

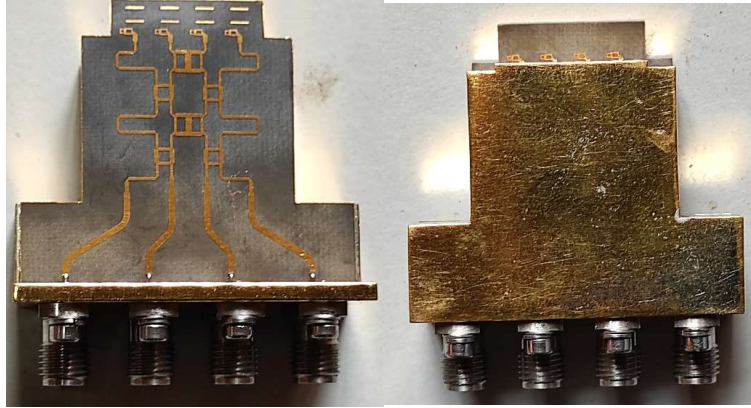


Figure 7. Fabricated prototype of RLDA array with BM.

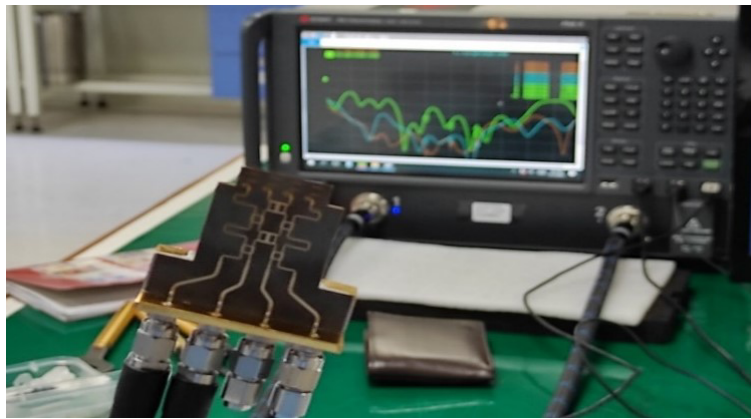


Figure 8. Test setup of proposed antenna with PNA-X N5244B (10 MHz–43.5 GHz) network analyzer.

neighbouring antenna elements when Port2 and Port3 are excited, which results in tilting the direction of the main beam of the antenna to -45° and $+45^\circ$ in the E -plane with respect to end-fire direction [21].

A prototype of the proposed design was fabricated on RT duroid-5880 material whose ϵ_r is 2.2, and the thickness is 10 mil as shown in Fig. 7. The fabricated array was fed by a 2.92 mm SMA connector with a supported assembly and tested on PNA-X N5244B (10 MHz–43.5 GHz) Network Analyzer. Prior to testing, Network Analyzer was electronically calibrated (Ecal) by Keysight N4693D Ecal module, and CRYSTEK 40 GHz cables were used to connect the fabricated antennas, as shown in Fig. 8. The reflection parameters over operating frequency band are below 16 dB and 13 dB, respectively, when Ports1,4 and Ports2,3 are excited, and the same are depicted in Fig. 9(a). The isolation between the ports is below 20 dB over operating frequency as seen in Fig. 9(b).

The radiation pattern measurement setup in an anechoic chamber is shown in Fig. 10. When testing is carried out, one of the four input ports is active, while the other ports are connected to 50Ω load. The measured results show that the four generated beams at 33.5 GHz are in the directions of 12° , -44° , 36° , and -14° with successive input port excitation and are acceptable with simulations as depicted in Fig. 11(a). Results for other frequencies are shown in Fig. 11(b) and Fig. 11(c).

Finally, the measured and simulated normalized radiation patterns at the three frequencies of 33.5, 34.5, and 35.5 GHz, when input ports P_1 – P_4 are excited, are summarized, as listed in Table 2. As observed from Table 2, $\pm 4^\circ$ variation is in the simulated and measured values for beam directions for respective input port excitations at 33.5, 34.5, and 35.5 GHz, which may be attributed to the losses from the connectors and measurement uncertainties.

Table 2. Simulated and measured beam directions for respective input port excitation.

Frequency	Excited port	Simulated Beam Direction (degree)	Measured Beam Direction (degree)
33.5 GHz	Port1	15	12
	Port2	-40	-44
	Port3	37	36
	Port4	-14	-14
34.5 GHz	Port1	14	13
	Port2	-36	-42
	Port3	40	37
	Port4	-15	-14
35.5 GHz	Port1	14	13
	Port2	-41	-43
	Port3	36	36
	Port4	-14	-14

Table 3. Comparison of intended work to past literature.

Ref	Frequency	Antenna type	Butler matrix	Number of layers	Maximum Beam steering (deg)	Area (mm ²)
[15]	60 GHz	1 × 4 patch	4 × 4 microstrip	1	40	3.6λ × 3.6λ = 12.96λ ²
[17]	30 GHz	1 × 4 Horn	4 × 4 microstrip	1	42	5λ × 5.2λ = 26λ ²
[18]	28 GHz	4 × 7 patch	4 × 4 microstrip	1	40	8.878λ × 2.99λ = 26.55λ ²
[19]	28 GHz	1 × 8 slot antenna	4 × 8 SIW	2	45	6.1λ × 4.1λ = 25.01λ ²
[20]	38 GHz	8 × 10 SIW slot-coupled patch array	Multifolded 4 × 8 Butler matrix	3	36	8.16λ × 7.6λ = 62λ ²
In this work	33.5–35.5 GHz	1 × 4 RLDA	4 × 4 microstrip	1	42	3.03λ × 3.03λ = 9.18λ ²

The designed switched beam antenna system comparison with previous works reported in the literature is summarized in Table 3. It is clearly observed that the overall dimensions of presented switched beam configuration are less than reported similar works [15,17]. Maximum beam steering is achieved in the proposed work in comparison with the other techniques already reported in the literature [18–20], although in some of the works more beam steering is achieved using complex structures SIW and multilayers. Moreover, in this work a novel high gain end-fire RLDA with quasi Yagi-Uda concept is used as radiating element which covers more band than other reported works.

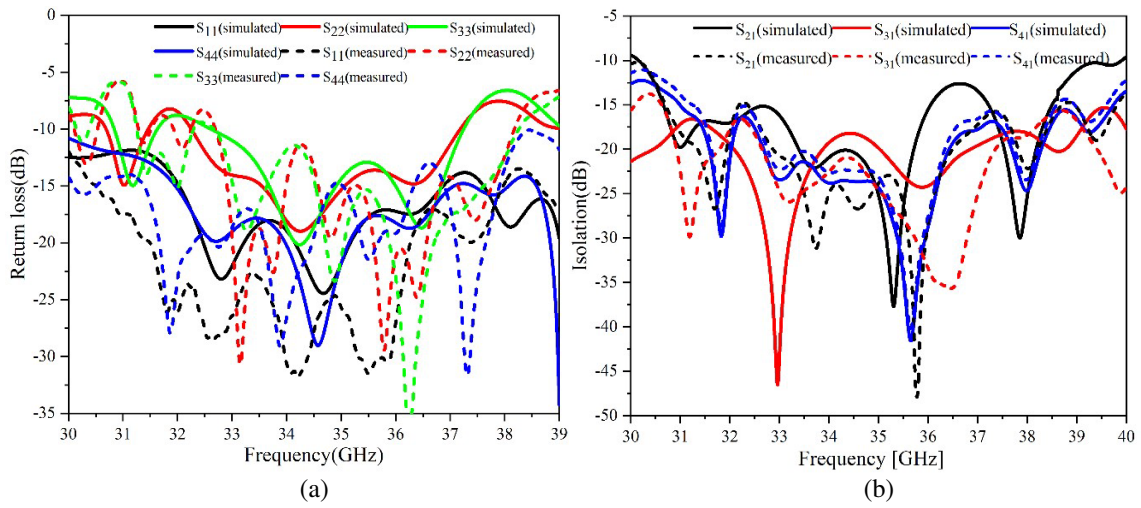


Figure 9. (a) Return loss. (b) Isolation of RLDA with BM.

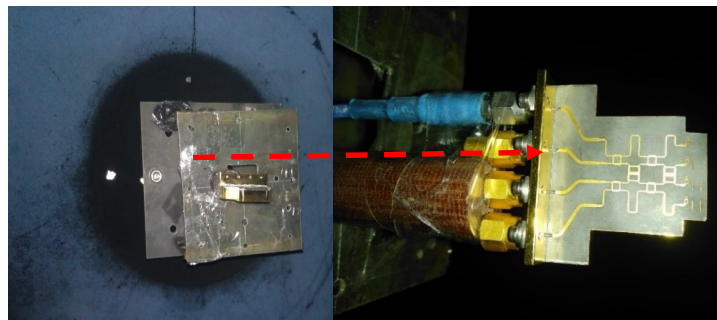
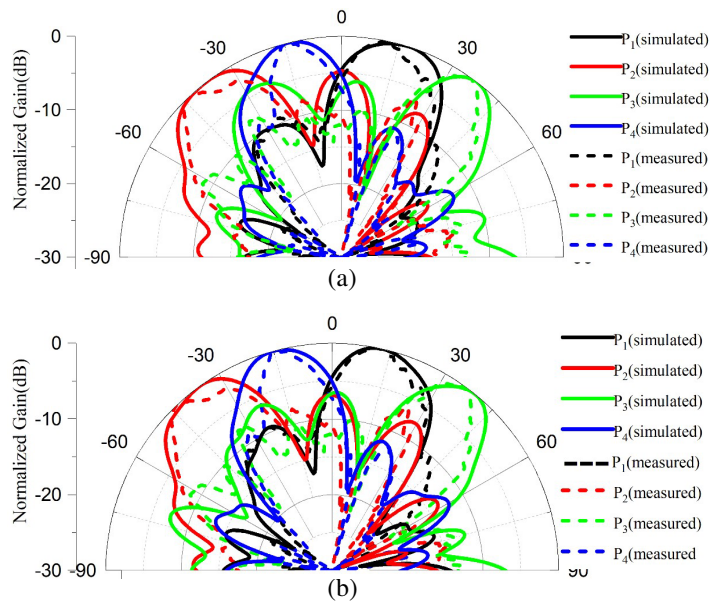


Figure 10. Pattern measurement of antenna in the anechoic chamber.



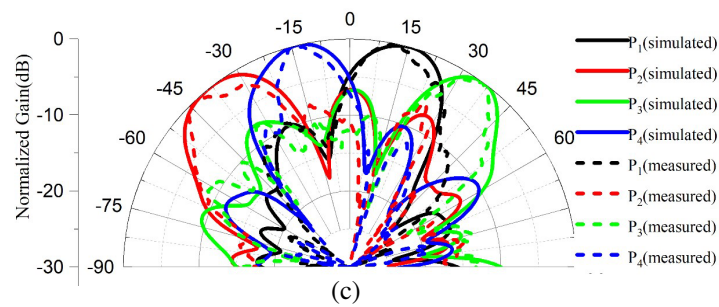


Figure 11. Normalized gain pattern at (a) 33.5 GHz, (b) 34.5 GHz, (c) 35.5 GHz.

5. CONCLUSION

A novel wideband high gain end-fire rectangular loop dipole antenna (RLDA) with quasi Yagi-Uda concept is presented with a 4×4 Butler matrix at mm-wave frequencies for switched beam applications. A prototype of the switched beam antenna configuration was fabricated, tested, and the measurements were compared with simulation results. In comparison to other reported works, this switched beam antenna configuration takes up less space and covers a wider band. The beam switching capability with good radiation performance makes this antenna suitable for current wireless communications and automotive sensor applications.

ACKNOWLEDGMENT

We would like to express our gratitude to Astra Microwave Private Limited, Hyderabad, India, for assisting in the antenna development and also thank to DLRL, DRDO, Hyderabad, India, for providing test and measurement facilities.

REFERENCES

1. Rappaport, T. S., et al., "Millimeter wave mobile communications for 5G cellular: It will work!," *IEEE Access*, Vol. 1, 335–349, 2013, doi: 10.1109/ACCESS.2013.2260813.
2. Abumunshar, A. J., K. Sertel, and N. K. Nahar, "Millimeter-wave tightly-coupled phased array with integrated MEMS phase shifters," *Progress In Electromagnetics Research C*, Vol. 110, 135–150, 2021.
3. Dadgarpour, B. Z., B. S. Virdee, and T. A. Denidni, "Beam tilting antenna using integrated metamaterial loading," *IEEE Transactions on Antennas and Propagation*, Vol. 62, No. 5, 2874–2879, May 2014, doi: 10.1109/TAP.2014.2308516.
4. Mantash, M., A. Kesavan, and T. A. Denidni, "Beam-tilting endfire antenna using a single-layer FSS for 5G communication networks," *IEEE Antennas and Wireless Propagation Letters*, Vol. 17, No. 1, 29–33, Jan. 2018, doi: 10.1109/LAWP.2017.2772222.
5. Dale Ake, W., M. Pour, and A. Mehrabani, "Asymmetric half-bowtie antennas with tilted beam patterns," *IEEE Transactions on Antennas and Propagation*, Vol. 67, No. 2, 738–744, Feb. 2019, doi: 10.1109/TAP.2018.2880078.
6. Mosca, S., F. Bilotti, A. Toscano, and L. Vegni, "A novel design method for Blass matrix beamforming networks," *IEEE Transactions on Antennas and Propagation*, Vol. 50, No. 2, 225–232, Feb. 2002, doi: 10.1109/8.997999.
7. Fakoukakis, F. and G. Kyriacou, "Novel nolen matrix based beamforming networks for series-fed low SLL multibeam antennas," *Progress In Electromagnetics Research B*, Vol. 51, 33–64, 2013.

8. Rahimian, A., Y. Alfadhil, and A. Alomainy, "Design and performance analysis of millimetre-wave Rotman lens-based array beamforming networks for large-scale antenna subsystems," *Progress In Electromagnetics Research C*, Vol. 78, 159–171, 2017.
9. Lian, J., Y. Ban, Z. Chen, B. Fu, and C. Xiao, "SIW folded Cassegrain lens for millimeter-wave multibeam application," *IEEE Antennas and Wireless Propagation Letters*, Vol. 17, No. 4, 583–586, Apr. 2018, doi: 10.1109/LAWP.2018.2804923.
10. Butler, J. and R. Lowe, "Beam-forming matrix simplifies design of electronically scanned antennas," *Electronic Design*, Vol. 9, 170–173, Apr. 12, 1961.
11. Panduro, M. A. and C. del Río-Bocio, "Simplifying the feeding network for multibeam circular antenna arrays by using corps," *Progress In Electromagnetics Research Letters*, Vol. 21, 119–128, 2011.
12. Panduro, M. A. and C. del Río-Bocio, "Design of beam-forming networks using CORPS and evolutionary optimization," *International Journal of Electronics and Communications*, Vol. 63, No. 5, 353–365, 2009, doi: 10.1016/j.aeue.2008.02.009.
13. Panduro, M. A. and C. del Río-Bocio, "Design of beam-forming networks for scannable multi-beam antenna arrays using CORPS," *Progress In Electromagnetics Research*, Vol. 84, 173–188, 2008.
14. Juárez, E., M. A. Panduro, A. Reyna, D. H. Covarrubias, A. Mendez, and E. Murillo, "Design of concentric ring antenna arrays based on subarrays to simplify the feeding system," *Symmetry*, Vol. 12, No. 6, 970, Jun. 2020, <https://doi.org/10.3390/sym12060970>.
15. Tseng, C., C. Chen, and T. Chu, "A low-cost 60-GHz switched-beam patch antenna array with butler matrix network," *IEEE Antennas and Wireless Propagation Letters*, Vol. 7, 432–435, 2008, doi: 10.1109/LAWP.2008.2001849.
16. Karamzadeh, S., V. Rafiei, and M. Kartal, "Beam steering fabry perot array antenna for MM-wave application," *Progress In Electromagnetics Research M*, Vol. 91, 81–89, 2020.
17. Ashraf, N., A.-R. Sebak, and A. A. Kishk, "PMC packaged single-substrate 4×4 butler matrix and double-ridge gap waveguide horn antenna array for multibeam applications," *IEEE Transactions on Microwave Theory and Techniques*, Vol. 69, No. 1, 248–261, Jan. 2021, doi: 10.1109/TMTT.2020.3022092.
18. Trinh-Van, S., J. M. Lee, Y. Yang, K. Lee, and K. C. Hwang, "A sidelobe-reduced, four-beam array antenna fed by a modified 4×4 butler matrix for 5G applications," *IEEE Transactions on Antennas and Propagation*, Vol. 67, No. 7, 4528–4536, Jul. 2019, doi: 10.1109/TAP.2019.2905783.
19. Lian, J., Y. Ban, C. Xiao, and Z. Yu, "Compact substrate-integrated 4×8 butler matrix with sidelobe suppression for millimeter-wave multibeam application," *IEEE Antennas and Wireless Propagation Letters*, Vol. 17, No. 5, 928–932, May 2018, doi: 10.1109/LAWP.2018.2825367.
20. Cao, Y., K. Chin, W. Che, W. Yang, and E. S. Li, "A compact 38 GHz multibeam antenna array with multifolded butler matrix for 5G applications," *IEEE Antennas and Wireless Propagation Letters*, Vol. 16, 2996–2999, 2017, doi: 10.1109/LAWP.2017.2757045.
21. Balanis, C. A., *Antenna Theory — Analysis and Design*, 3rd Edition, John Wiley & Sons, Inc., 2005.